analytical chemistry

Article

pubs.acs.org/ac

Detection of Adenosine Triphosphate with an Aptamer Biosensor Based on Surface-Enhanced Raman Scattering

Ming Li,[†] Jianming Zhang,[‡] Savan Suri,[†] Letha J. Sooter,[§] Dongling Ma,[‡] and Nianqiang Wu*[,†]

[†]Department of Mechanical and Aerospace Engineering, WVNano Initiative, West Virginia University, Morgantown, West Virginia 26506-6106, United States

[‡]Institut National de la Recherche Scientifique (INRS), Énergie, Matériaux et Télécommunications, 1650 Boulevard Lionel-Boulet, Varennes, Québec J3X 1S2, Canada

[§]Department of Basic Pharmaceutical Sciences, WVNano Initiative, West Virginia University, Morgantown, West Virginia 26506-9530, United States

Supporting Information

ABSTRACT: A simple, ultrasensitive, highly selective, and reagent-free aptamer-based biosensor has been developed for quantitative detection of adenosine triphosphate (ATP) using surface-enhanced Raman scattering (SERS). The sensor contains a SERS probe made of gold nanostar@Raman label@SiO_2 core–shell nanoparticles in which the Raman label (malachite green isothiocyanate, MGITC) molecules are sandwiched between a gold nanostar core and a thin silica shell. Such a SERS probe brings enhanced signal and low background fluorescence, shows good water-solubility and stability, and exhibits no sign of photobleaching. The aptamer labeled with the SERS probe is designed to hybridize with the cDNA on a gold film to form a rigid duplex DNA. In the presence of ATP, the interaction between ATP and the aptamer results in the dissociation of the duplex DNA structure and thereby removal of the SERS probe from the gold film, reducing the Raman signal. The response of the SERS biosensor varies linearly with the logarithmic ATP concentration up to 2.0 nM with a limit of detection of 12.4 pM. Our work has provided an effective method for detection of small molecules with SERS.

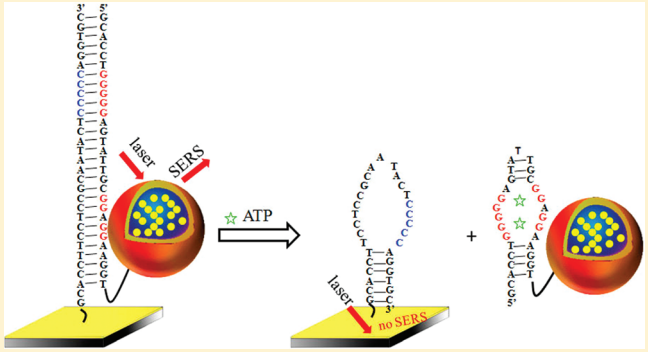

Development of rapid and sensitive methods for detection of small organic molecules such as cocaine, 2,4,6-trinitrotoluene (TNT), dopamine, and adenosine is highly desirable for environmental detection, forensic services as well as medical diagnostics and therapeutics. Several strategies including Förster resonance energy transfer (FRET),[1,2] colorimetric response,[3−6] electrochemical analyses,[7−10] and optical surface plasmon resonance[11] have been demonstrated for quantitative detection of small molecules. However, it still remains challenging to develop small molecule sensors in terms of sensitivity, assay time, reproducibility, and on-site applicability. Surface-enhanced Raman spectroscopy (SERS) has emerged as an alternative tool for biosensing because of its unique features,[12−18] including (i) providing spectral fingerprinting information of molecules, (ii) multiplexed detection capability with a single laser excitation resulting from the narrow line width of vibrational Raman bands, (iii) high sensitivity with a potential of single molecule detection, and (iv) easy operation without complicated sample preparation, rendering on-site, nondestructive detection in a wide variety of matrices. Therefore, SERS has been employed as an efficient sensing method for detection of viruses, DNA, TNT, and heavy metallic ions.[19−28]

In typical SERS assays, Raman reporters are directly attached to the surface of metallic nanoparticles (the SERS substrates) to provide the Raman signal.[20] These Raman reporters are vulnerable to detachment from the surface of metallic nanoparticles upon direct exposure to the environment, leading to poor reproducibility of SERS sensing. Also, the metallic nanoparticles labeled with Raman reporters have poor water-solubility and tend to aggregate in the aqueous matrix containing analytes. Moreover, the commonly used SERS substrates such as gold or silver nanoparticles are typically covered by the surface ligands that are inherent from the synthesis process, which may be unfavorable for surface bioconjugation. Therefore, a protective shell has been used to wrap a combination of the metallic SERS substrates and the Raman reporter. This prevents from leaching-out of the Raman reporters and improves their water-solubility and stability as well as the reproducibility of the SERS signals.[24,29,30]

In the present work, the gold nanostar@Raman label@SiO_2 nanoparticles are produced by sandwiching the Raman reporter

Received: December 14, 2011
Accepted: February 15, 2012
Published: February 29, 2012

dx.doi.org/10.1021/ac203325z | *Anal. Chem.* 2012, 84, 2837−2842

(malachite green isothiocyanate, MGITC) molecules between a gold nanostar core and a thin silica shell. MGITC was chosen as the Raman label due to its nonfluorescent characteristic and its isothiocyanate (—N═C═S) group that can both bind to the gold surface and is compatible with the SiO_2 encapsulation process as well.[2,10] SiO_2 is employed as a protective layer because of its long-term stability and easy bioconjugation. Raman scattering is extremely inefficient due to the limited scattering cross section of $\sim 10^{-30}$ cm^2/molecule, which is about 14 orders of magnitude lower than the absorption cross sections of fluorescent dye molecules.[11] Therefore, the gold nanostars were used as the Raman substrate, because they have been shown to have very high electromagnetic enhancement for SERS due to the rough surface, as opposed to the smooth, round-shaped SERS substrates.[31−34] The gold nanostar@MGITC@SiO_2 nanoparticles act as a highly sensitive SERS probe that features high sensitivity, good water-solubility and stability, low background fluorescence, and strong resistance to photobleaching for biological applications. Here, such a SERS probe is employed for detection of adenosine triphosphate (ATP), a universal energy carrier in biological systems that plays a crucial role in the regulation of cellular metabolism and biochemical pathways in cell physiology.[35] To recognize ATP specifically, a specific aptamer developed previously[36] is chosen as the capture probe. In the present SERS biosensor, the aptamer labeled with the gold nanostar@MGITC@SiO_2 nanoparticles are initially immobilized on a gold film. This assembly exhibits a strong SERS signal. Upon addition of ATP into the assay, the gold nanostar@MGITC@SiO_2-labeled aptamer detachs from the gold film, which "turns off" the Raman signal on the gold film. As a result, an ultrasensitive and highly selective ATP biosensor has been developed.

EXPERIMENTAL SECTION

Chemicals and Reagents. Malachite green isothiocyanate (MGITC) was purchased from Molecular Probes, Inc. 3-Triethoxysilylpropyl succinic anhydride (TEPSA) was purchased from Gelest Inc. DNA sequences of 3′-NH_2-$(CH_2)_3$-TGG AAG GAG GCG TTA TGA GGG GGT CCA CG-5′ and 5′-NH_2-$(CH_2)_6$-GCA CCT TCC TCC GCA ATA CTC CCC CAG GTG C-3′ were synthesized by Eurofins MWG Operon (Huntsville, AL) according to the sequences reported previously.[36,37] Na_2HPO_4 (99.0%) and NaH_2PO_4 (99.0%) came from Alfa Aesar. *N*-Hydroxysuccinimide (NHS), 1-ethyl-3-(3-dimethylaminopropyl)-carbodiimide (EDC), 11-mercaptoundecanoic acid (MUA), 11-mercapto-1-undecanol ethanolic (MU), adenosine triphosphate (ATP), cytidine triphosphate (CTP), and guanosine triphosphate (GTP) were purchased from Sigma-Aldrich. All solvents were of analytical grade and used without further purification. Deionized (D.I.) water was purified using a Milli-Q Millipore system (18.2 MΩ/cm,[2] Millipore Corp.).

Apparatus. The nanoparticles were observed with a field-emission JEOL JSM-7600F scanning electron microscope (SEM) and a JEOL JEM-2100F transmission electron microscope (TEM) at an acceleration voltage of 200 kV. UV−visible absorption spectra were acquired in a range of 200−900 nm by a Shimadzu UV-2550 spectrometer. Raman measurements were conducted in a Renishaw InVia Raman spectrometer at an excitation laser of 532 nm. A microscope equipped with a 20× objective was used to focus the incident excitation laser. The laser power on the sample was 50 mW, and the accumulation time was 10 s. The Raman spectra were calibrated and normalized with Si. Fourier transform infrared (FT-IR) spectra were obtained with the attenuated total reflection (ATR) mode in a Thermo Nicolet 6700 spectrometer. X-ray photoelectron spectroscopy (XPS) was performed with a PHI 5000 Versa Probe system (Physical Electronics, MN). The XPS spectra were calibrated with the reference to the C 1s peak of aliphatic carbon at 284.8 eV.

Synthesis of Gold Nanostar@MGITC@SiO_2 Sandwich Nanoparticles. First, the gold nanostar was synthesized according to the procedure described below. Briefly, $HAuCl_4 \cdot 3H_2O$ aqueous solution (1 mL, 1 wt %) was first diluted with 90 mL of water, followed by the injection of trisodium citrate (2 mL, 38.8 mM). Subsequently, freshly prepared $NaBH_4$ solution (1 mL, 0.075 wt % in 38.8 mM trisodium citrate solution) was added, and then, the reaction mixture was kept at room temperature overnight with constant stirring to form the seed solution. Following this, 50 mL of the gold seed solution was mixed with poly(vinyl pyrrolidone) (PVP, 10 mM) at room temperature for 24 h to prepare the PVP-coated gold seed solution. Finally, 82 μL of 50 mM $HAuCl_4$ aqueous solution was mixed with 15 mL of 10 mM PVP in dimethylformamide, followed by the rapid addition of 43 μL of the PVP-coated gold seed solution ([Au] ≈ 4 mM) with constant stirring at room temperature for 13 h.

For SiO_2 coating, the absorbance of the nanostars was adjusted by D.I. water to 2.5 at the longer surface plasmon peak. After this, 5.0 μL of the MGITC aqueous solution was added to 1 mL of purified nanostar solution and then stirred for 30 min before adding 50 μL of fresh MPTMS solution (50 mM) and continuing constant stirring for additional 30 min. Subsequently, 100 μL of fresh sodium silicate solution (0.54 wt %, pH > 12) was added and was stirred for 10 min, and then, it was kept undisturbed for one day before adding 1 mL of anhydrous ethanol to generate a condensed SiO_2 layer. The resulting solution was centrifuged and washed with anhydrous ethanol. The precipitates were redispersed in D.I. water for future use.

DNA Functionalization of Gold Nanostar@MGITC@SiO_2. TEPSA (200 μL, 200 mM) was added to 400 μL of gold nanostar@MGITC@SiO_2 aqueous solution and then incubated overnight. COOH-terminated gold nanostar@MGITC@SiO_2 was achieved after centrifugation and redispersed in 200 μL of phosphate buffered saline (PBS) solution (10 mM Na_2HPO_4/NaH_2PO_4, pH = 7.0) for future use. The functionalization of DNA was carried out by the carbodiimide chemistry.[38] First, 100 μL of solution containing 50 mM NHS and 200 mM EDC was added to the gold nanostar@MGITC@SiO_2 solution to activate the COOH group. After incubation for 2 h, 50 μL of 0.1 mM DNA sequence of 3′-NH_2-$(CH_2)_3$-TGG AAG GAG GCG TTA TGA GGG GGT CCA CG-5′ (aptamer, Signaling Probe) was added. After standing overnight, the solution was centrifuged and washed using a PBS solution to obtain the aptamer-functionalized particles, which were dispersed in 800 μL of PBS solution for future use.

Preparation of ssDNA-Modified Substrates. The gold films were prepared by vapor deposition on the Si substrates with a thin Cr layer as the adhesion layer. The resulting gold film was cleaned by successive immersion in CH_2Cl_2, ethanol, and D.I. water for 10 min, respectively, and heated at 90 °C in 20 mL of peroxide solution for 1 h. Following this, the gold films were successively washed with ethanol and D.I. water, respectively, and dried at 60 °C in a vacuum oven. The cleaned gold films were incubated overnight in a solution containing

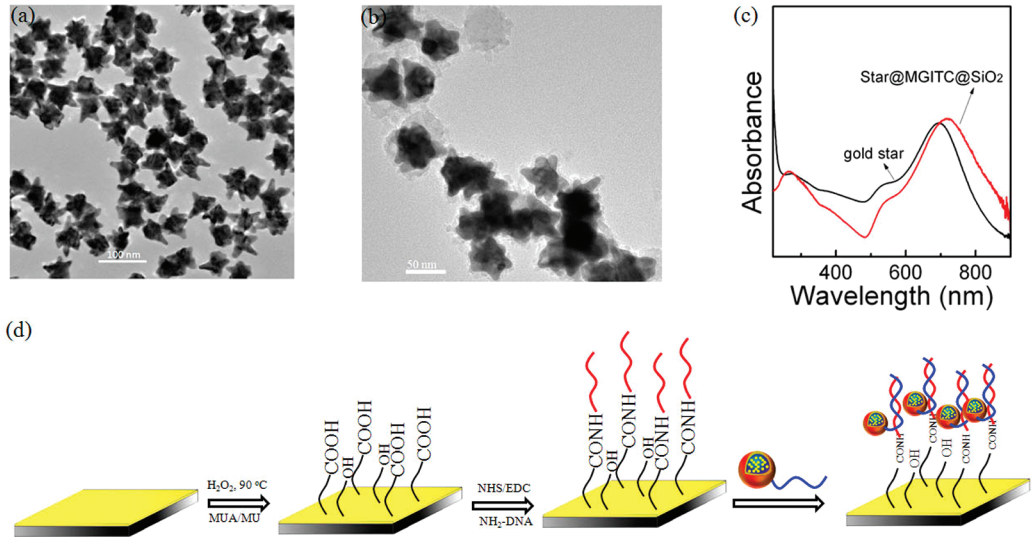

Figure 1. TEM images of the bare gold nanostars (a) and the gold nanostar@MGITC@SiO_2 sandwich nanoparticles (b); UV−visible absorption spectra (c); schematic illustration of the SERS sensor assembly (d).

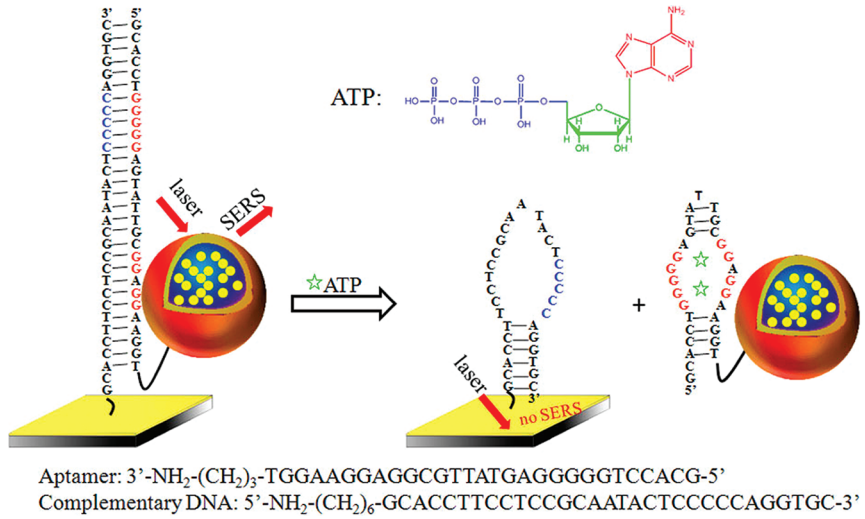

Figure 2. Operation principle of the SERS sensor for ATP detection. The molecular structure of the ATP and DNA sequences are shown.

100 mM MUA and 100 mM MU and then washed using ethanol and D.I. water, respectively. The resulting MUA/MU-modified gold film was activated by immersion in a solution containing 50 mM NHS and 200 mM EDC in a PBS solution. The activated MUA/MU-modified gold film was incubated overnight in a PBS solution containing 0.1 mM DNA with sequence of 5′-NH_2-$(CH_2)_6$-GCA CCT TCC TCC GCA ATA CTC CCC CAG GTG C-3′ (Capture Probe). After immobilization of the cDNA, the gold film was successively rinsed with D.I. water and PBS solution to remove free and excess DNA.

Assembly of SERS Sensor for ATP Detection. The cDNA-modified gold substrates were immersed in the aptamer-functionalized gold nanostar@MGITC@SiO_2 solution obtained above. After incubation at 40 °C in a water bath for 1 h, the gold films were washed with the PBS solution. The resulting substrates were modified by double-stranded DNA (dsDNA) labeled with gold nanostar@MGITC@SiO_2 as the signaling probe.

For ATP detection, the SERS sensors were immersed in a PBS solution (10 mM PBS, 0.3 M NaCl, pH = 7) containing various concentrations (0−1 μM) of ATP (CTP or GTP) and incubated for 30 min. The SERS sensors were then rinsed by 10 mM PBS. Subsequently, the Raman spectra were acquired from the substrates for an accumulation time of 10 s. Three spectra from different sites were collected from each sample and averaged to represent the SERS results.

RESULTS AND DISCUSSION

Figure 1a,b shows the TEM images of the gold nanostars before and after coating of a ∼5 nm thick SiO_2 layer, respectively. Figure 1c reveals the UV−visible absorption spectra of the bare gold nanostars and the gold nanostar@MGITC@SiO_2 composite nanoparticles in an aqueous solution. A localized surface plasmon resonance (LSPR) absorption band at 697 nm was observed for the bare gold nanostar while a LSPR band at 715 nm was seen for the gold nanostar@MGITC@SiO_2 sandwich nanoparticles. The red-shift of the LSPR peak may be ascribed to the higher refractive index of SiO_2 with respect to that of water.

Figure 1d shows the assembly procedure of the SERS sensor used for ATP detection. The carboxylic acid-terminated MUA

dx.doi.org/10.1021/ac203325z | Anal. Chem. 2012, 84, 2837−2842

and MU molecules were anchored on the gold film via the S−Au linkage. The amine terminated, single-stranded (ss) DNA (capture probe) was immobilized on the carboxyl functionalized gold film via the carbodiimide chemistry. The complementary ssDNA aptamer (signaling probe) labeled with the gold nanostar@MGITC@SiO_2 nanoparticles was assembled on the surface via hybridization with the preimmobilized ssDNA (capture probe). As a result, the gold nanostar@MGITC@SiO_2 nanoparticles were immobilized on the gold film, leading to the formation of a SERS sensor used for ATP detection. To ensure the sensor assembly quality, each step of the sensor assembly was tracked by acquisition of the FT-IR and the XPS spectra,[39−42] as shown in Supporting Information (Figures S1 and S2).

Figure 2 shows the operation process of the SERS sensor for ATP detection. The gold nanostar@MGITC@SiO_2 nanoparticles were initially immobilized on the gold film surface via the duplex DNA. A high density of nanoparticles was observed on the gold film surface under SEM (Figure 3). Under the laser

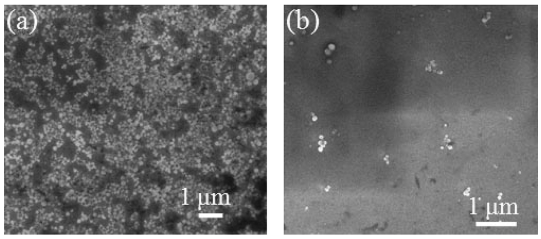

Figure 3. SEM images of the SERS sensor system based on the gold nanostar@MGITC@SiO_2 nanoparticles before (a) and after exposure to 100 nM ATP (b).

excitation, the strong SERS signal from the immobilized nanoparticles was detected (Figure 4b). The assignments of the

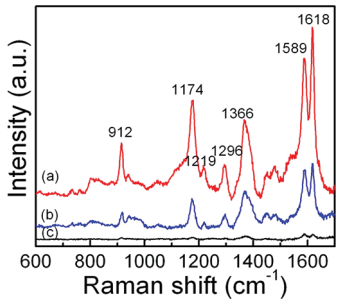

Figure 4. Raman spectra obtained from the gold nanostar@MGITC@SiO_2 in solution (a), the SERS sensor before exposure to the ATP solution (b), and the SERS sensor after exposure to 100 nM ATP solution (c).

Raman bands in Figure 4b are listed in Table S1 in Supporting Information. The peaks at 1618, 1589, and 1366 cm^{-1} were attributed to the phenyl-N stretching mode, the in-plane ring stretching and bending modes, and the aromatic ring stretching mode, respectively.[43,44] The peaks at 1296, 1174, and 912 cm^{-1} were ascribed to the in-plane C−H or C−C−H bending mode, the in-plane benzene v_9 mode, and the B_{1u} in-plane benzene ring mode, respectively.[43,44] When the ATP molecules were added into the SERS assay, the ATP molecules interacted with the aptamer labeled with the gold nanostar@MGITC@SiO_2 (signaling probe). Two ATP molecules were intercalated into each aptamer by forming the noncanonical G/A base pairs,[36,45] leading to the dissociation of the duplex DNA (Figure 2). Consequently, the aptamer labeled with the gold nanostar@MGITC@SiO_2 (signaling probe) was detached from the gold film surface. The SEM image (Figure 3b) confirmed that only a negligible amount of nanoparticles remained on the gold film surface after the SERS sensor had been incubated in the 100 nM ATP solution and rinsed with the PBS solution. As a result, the significantly reduced Raman signal was obtained from the gold film surface (Figure 4c).

Figure 5 shows the response of the SERS sensor to the variation of the ATP concentration in the PBS solution. At a

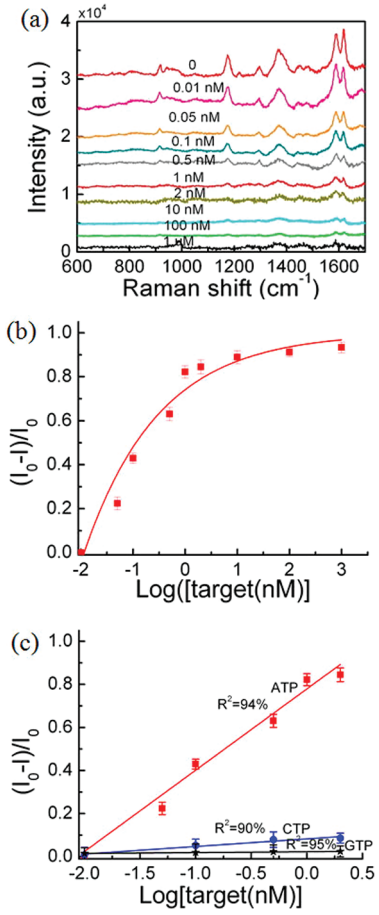

Figure 5. (a) SERS spectra of the Raman label in the SERS sensor; (b) sensor response versus the logarithmic concentration of ATP; (c) the linear range of the sensor response to ATP, CTP, and GTP.

low ATP concentration, the SERS spectra were characteristic of MGITC molecules, which were consistent with Figure 4b. The intensity of all the Raman peaks decreased with increasing ATP concentration (Figure 5a). No evident Raman peak associated with MGITC was observed as the ATP concentration reached 10 nM, which indicated that almost all nanoparticles were removed from the gold film surface. The normalized response $[i = (I_0 - I)/I_0]$ of the Raman peak intensity at 1618 cm^{-1} was plotted as a function of the ATP concentration on a logarithmic scale (Figures 5b). I_0 and I were the intensities of the Raman peak in the absence and the presence of ATP, respectively. The limit of detection (LOD), which was defined as three times the standard deviation of the blank, was determined to be 12.4 pM. This LOD value was much lower than that obtained from previous electrochemical,[8,10] fluorescent, and colorimetric

dx.doi.org/10.1021/ac203325z | Anal. Chem. 2012, 84, 2837−2842

methods[37,46−48] with aptamers as the molecular recognition elements. The sensor response (i) became saturated when the ATP concentration reached 10 nM. Furthermore, a linear range of the sensor response versus the log[ATP] was 12.4 pM to 2.0 nM as shown in Figure 5c.

The SERS biosensor developed in this work exhibits a very low LOD. This is due to the following three reasons. First, the unique shape of the gold nanostars leads to significant enhancement of the local electromagnetic field surrounding the surface of the Au nanostars. Second, the sandwich-structured nanoparticles are immobilized in proximity to the gold film surface by utilizing the rigid feature of dsDNA and the intentionally designed orientation of the signaling probes. In this architecture, "hot spots" are formed between the gold nanostars and the gold film, leading to SERS enhancement. If the gold nanostars are distal from the gold film surface, the SERS enhancement effect will be diminished. Third, the DNA aptamer has a high affinity with ATP.[37] That is, the combination of aptamer with ATP can lead to a much lower free energy system.

In order to evaluate the specificity of the SERS sensor toward ATP, control experiments were conducted by incubating the SERS sensor in the PBS solution containing various concentrations of GTP or CTP, respectively (Figure 5c). It can also be seen that exposure to different concentrations of GTP and CTP induced a negligible response of the SERS sensor although GTP and CTP have the chemical structures similar to ATP (See Figures S3−S4 in Supporting Information).

CONCLUSIONS

In summary, an ultrasensitive SERS sensor was developed for detection of ATP, in which the aptamer was employed as the molecular recognition element and the gold nanostar@MGITC@SiO_2 nanoparticle as the signaling probe. The SERS sensor exhibited good specificity and high sensitivity toward the ATP molecules with a limit of detection of 12.4 pM. The gold nanostars acted as the SERS substrate with large signal amplification ability, yielding high sensitivity of the SERS sensor. Encapsulation of a large number of MGITC molecules inside the sandwich-structured nanoparticles also contributed to the high sensitivity. Furthermore, the gold nanostar@MGITC@SiO_2 sandwiched structure gave the stability and the reproducibility of the sensing assay.

ASSOCIATED CONTENT

Supporting Information

Figures S1−S4 and Table S1. This material is available free of charge via the Internet at http://pubs.acs.org.

AUTHOR INFORMATION

Corresponding Author

*Fax: (304)-293-6689. E-mail: nick.wu@mail.wvu.edu.

Notes

The authors declare no competing financial interest.

ACKNOWLEDGMENTS

The resource and facilities used were partially supported by NSF (EPS 1003907) and a Research Challenge Grant from the State of West Virginia (EPS08-01), the West Virginia University Research Corporation, and the West Virginia EPSCoR Office. D.M. is grateful to the financial support from the Natural Sciences and Engineering Research Council of Canada and Fonds de la recherche sur la nature et les technologies. We are grateful to Dr. W. Ding for assistance of the share facility operation.

REFERENCES

(1) Goldman, E. R.; Medintz, I. L.; Whitley, J. L.; Hayhurst, A.; Clapp, A. R.; Uyeda, H. T.; Deschamps, J. R.; Lassman, M. E.; Mattoussi., H. *J. Am. Chem. Soc.* **2005**, *127*, 6744−6751.
(2) Endoh, T.; Shintani, R.; Mie, M.; Kobatake, E.; Ohtsuki, T.; Sisido, M. *Bioconjugate Chem.* **2009**, *20*, 2242−2246.
(3) Forzani, E. S.; Lu, D.; Leright, M. J.; Aguilar, A. D.; Tsow, F.; Iglesias, R. A.; Zhang, Q.; Lu, J.; Li, J.; Tao, N. J. *J. Am. Chem. Soc.* **2009**, *131*, 1390−1391.
(4) Xu, X.; Wang, J.; Yang, F.; Jiao, K.; Yang, X. *Small* **2009**, *5*, 2669−2672.
(5) Kong, B.; Zhu, A.; Luo, Y.; Tian, Y.; Yu, Y.; Shi, G. *Angew. Chem., Int. Ed.* **2011**, *50*, 1837 −1840.
(6) Jiang, Y.; Zhao, H.; Lin, Y.; Zhu, N.; Ma, Y.; Mao, L. *Angew. Chem., Int. Ed.* **2010**, *49*, 4800 −4804.
(7) Aguilar, A. D.; Forzani, E. S.; Leright, M.; Tsow, F.; Cagan, A.; Iglesias, R. A.; Nagahara, L. A.; Amlani, I.; Tsui, R.; Tao, N. J. *Nano Lett.* **2010**, *10*, 380−384.
(8) Zayats, M.; Huang, Y.; Gill, R.; Ma, C.; Willner, I. *J. Am. Chem. Soc.* **2006**, *128*, 13666−13667.
(9) Baker, B. R.; Lai, R. Y.; Wood, M. S.; Doctor, E. H.; Heeger, A. J.; Plaxco, K. W. *J. Am. Chem. Soc.* **2006**, *128*, 3138−3139.
(10) Zuo, X.; Xiao, Y.; Plaxco, K. W. *J. Am. Chem. Soc.* **2009**, *131*, 6944−6945.
(11) Wang, J.; Zhou, H. S. *Anal. Chem.* **2008**, *80*, 7174−7178.
(12) Li, M.; Li, R.; Li, C. M.; Wu, N. Q. *Front. Biosci.* **2011**, *3*, 1308−1331.
(13) Cao, Y. W. C.; Jin, R.; Mirkin, C. A. *Science* **2002**, *297*, 1536−1540.
(14) Nie, S.; Emory, S. R. *Science* **1997**, *275*, 1102−1106.
(15) Kim, N. H.; Lee, S. J.; Moskovits, M. *Nano Lett.* **2010**, *10*, 4181−4185.
(16) Tognalli, N. G.; Cortés, E.; Hernández-Nieves, A. D.; Carro, P.; Usaj, G.; Balseiro, C. A.; Vela, M. E.; Salvarezza, R. C.; Fainstein, A. *ACS Nano* **2011**, *5*, 5433−5443.
(17) Ochsenkühn, M. A.; Jess, P. R. T.; Stoquert, H.; Dholakia, K.; Campbell, C. J. *ACS Nano* **2009**, *3*, 3613−3621.
(18) Chen, G.; Wang, Y.; Yang, M.; Xu, J.; Goh, S. J.; Pan, M.; Chen, H. *J. Am. Chem. Soc.* **2010**, *132*, 3644−3645.
(19) Barhoumi, A.; Halas, N. J. *J. Am. Chem. Soc.* **2010**, *132*, 12792−12793.
(20) Dasary, S. S. R.; Singh, A. K.; Senapati, D.; Yu, H.; Ray, P. C. *J. Am. Chem. Soc.* **2009**, *131*, 13806−13812.
(21) Han, D.; Sung Lim, Y.; Kim, B. J.; Piao, L.; Chung, T. D. *Chem. Commun.* **2010**, *46*, 5587−5589.
(22) Wang, G.; Lipert, R. J. *Anal. Chem.* **2011**, *83*, 2554−2561.
(23) Papadopoulou, E.; Bell, S. E. J. *Angew. Chem., Int. Ed.* **2011**, *50*, 9058 −9061.
(24) Chen, X.; Liu, H.; Zhou, X.; Hu, J. *Nanoscale* **2011**, *2*, 2841−2846.
(25) Pallaoro, A.; Braun, G. B.; Reich, N. O.; Moskovits, M. *Small* **2010**, *6*, 618−622.
(26) Lee, S. J.; Moskovits, M. *Nano Lett.* **2011**, *11*, 145−150.
(27) Ochsenkühn, M. A.; Campbell, C. J. *Chem. Commun.* **2010**, *46*, 2799−2801.
(28) Shanmukh, S.; Jones, L.; Driskell, J.; Zhao, Y.; Dluhy, R.; Tripp, R. A. *Nano Lett.* **2006**, *6*, 2630−2636.
(29) Küstner, B.; Gellner, M.; Schütz, M.; Schöppler, F.; Marx, A.; Ströbel, P.; Adam, P.; Schmuck, C.; Schlücker, S. *Angew. Chem., Int. Ed.* **2009**, *48*, 1950−1953.
(30) Doering, W. E.; Nie, S. *Anal. Chem.* **2003**, *75*, 6171−6176.
(31) Nehl, C. L.; Liao, H.; Hafner, J. H. *Nano Lett.* **2006**, *6*, 683−688.

(32) Khoury, C. G.; Vo-Dinh, T. *J. Phys. Chem. C* **2008**, *112*, 18849−18859.
(33) Rodríguez-Lorenzo, L.; Álvarez-Puebla, R. A.; de Abajo, F. J. G.; Liz-Marzán, L. M. *J. Phys. Chem. C* **2010**, *114*, 7336−7340.
(34) Esenturk, E. N.; Walker, A. R. H. *J. Raman Spectrosc.* **2009**, *40*, 86−91.
(35) Ross, J. *J. Phys. Chem. B* **2006**, *110*, 6987−6990.
(36) Liu, J.; Cao, Z.; Lu, Y. *Chem. Rev.* **2009**, *109*, 1948−1998.
(37) Huizenga, D. E.; Szostak, J. W. *Biochemistry* **1995**, *34*, 656−665.
(38) Wang, H.; Xu, W.; Zhang, H.; Li, D.; Yang, Z.; Xie, X.; Li, T.; Liu, X. *Small* **2011**, *7*, 1987−1992.
(39) Wu, N.; Fu, L.; Su, M.; Aslam, M.; Wong, K. C.; Dravid, V. P. *Nano Lett.* **2004**, *4*, 383−386.
(40) Lim, M.; Feng, K.; Chen, X.; Wu, N. Q.; Raman, A.; Gawalt, E. S.; Nightingale, J.; Korakakis, D.; Hornak, L. A.; Timperman, A. *Langmuir* **2007**, *23*, 2444−2452.
(41) Socrates, G. *Infrared and Raman Characteristic Group Frequencies Tables and Charts*, 3rd ed.; John Wiley & Sons Ltd: London, 2001.
(42) Tunc, I.; Suzer, S.; Correa-Duarte, M. A.; Liz-Marzán, L. M. *J. Phys. Chem. B* **2005**, *109*, 7597−7600.
(43) Kamińska, A.; Dzięcielewski, I.; Weyher, J. L.; Waluk, J.; Gawinkowski, S.; Sashuk, V.; Fiałkowski, M.; Sawicka, M.; Suski, T.; Porowski, S.; Hołyst, R. *J. Mater. Chem.* **2011**, *21*, 8662−8669.
(44) Lueck, H. B.; Daniel, D. C.; McHale, J. L. *J. Raman Spectrosc.* **1993**, *24*, 363−370.
(45) Yao, W.; Wang, L.; Wang, H.; Zhang, X.; Li, L. *Biosens. Bioelectron.* **2009**, *24*, 3269−3274.
(46) Wang, Y.; Wang, Y.; Liu, B. *Nanotechnology* **2008**, *19*, 415605.
(47) Wang, J.; Jiang, Y.; Zhou, C.; Fang, X. *Anal. Chem.* **2005**, *77*, 3542−3546.
(48) Liu, F.; Zhang, J.; Chen, R.; Chen, L.; Deng, L. *Chem. Biodiversity* **2011**, *8*, 311−316.